Elucidation of the biodegradation pathways of bis(2-hydroxyethyl) terephthalate and dimethyl terephthalate under anaerobic conditions revealed by enrichment culture and microbiome analysis

Kyohei Kuroda[1*], Takashi Narihiro[1*], Yuki Nakaya[2], Taro Q.P. Noguchi[3], Ryota Maeda[3,4], Masaru K. Nobu[5], Yuki Ohnishi[6], Yasuhiro Kumaki[7], Tomoyasu Aizawa[6], Hisashi Satoh[2]

[1]Bioproduction Research Institute, National Institute of Advanced Industrial Science and Technology (AIST), 2-17-2-1 Tsukisamu-Higashi, Toyohira-ku, Sapporo, Hokkaido, 062-8517 Japan

[2]Division of Environmental Engineering, Faculty of Engineering, Hokkaido University, North-13, West-8, Hokkaido, 060-8628 Japan

[3]Department of Chemical Science and Engineering, National Institute of Technology, Miyakonojo College, 473-1 Yoshio-cho, Miyakonojo, Miyazaki, 885-8567 Japan

[4]Department of Frontier Science for Advanced Environment, Graduate School of Environmental Studies, Tohoku University, 6-6-06 Aramaki Aza Aoba, Aoba-ku, Sendai, Miyagi 980-8579, Japan

[5]Bioproduction Research Institute, National Institute of Advanced Industrial Science and Technology (AIST), Central 6, Higashi 1-1-1, Tsukuba, Ibaraki 305-8566 Japan

[6]Faculty of Advanced Life Science, Hokkaido University, North-10, West-8, Kita-ku, Sapporo, Hokkaido, 060-0810 Japan

[7]Faculty of Science, Hokkaido University, North-10, West-8, Kita-ku, Sapporo, Hokkaido, 060-0810 Japan

*Co-corresponding authors:

Takashi Narihiro, Tel: +81 29 861 9443; E-mail: t.narihiro@aist.go.jp

Kyohei Kuroda, Tel: +81 11 857 8402; E-mail: k.kuroda@aist.go.jp

Graphical Abstract

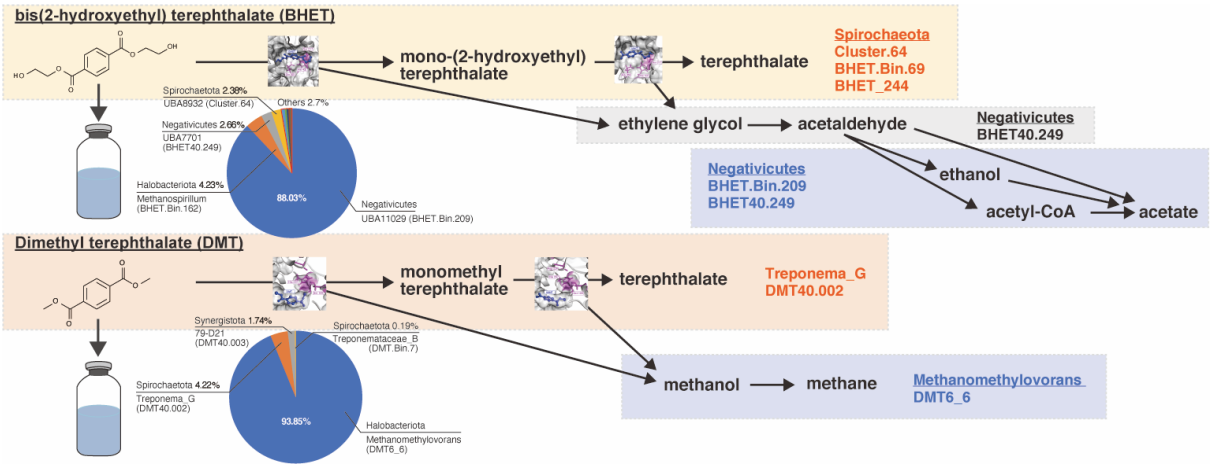

Highlights

· BHET- and DMT-degradation successfully took place under anaerobic condition.

· BHET- and DMT-degrading enzymes were predicted from members of Spirochaeota.

· BHET-derived byproducts were utilized by putative acetogens of the class Negativicutes.

· Methanol produced from DMT degradation was utilized by methanol-utilizing methanogens.

Abstract

With the globally rising usage of plastics, including polyethylene terephthalate (PET), the environmental risk that disposal of waste plastics to landfills and discharge of microplastics to the marine environment pose have also increased. For example, observation of animal ingestion of fragmented waste plastics (micro- and nano-plastics) has driven

awareness for the need of proper environmental risk assessment. In evaluating the biodegradability of PET-derived byproducts and their precursors, most work has focused on hydrolytic enzymes and aerobic organisms that possess such genes, but only few reports on biodegradation in the absence of oxygen (*i.e.*, anaerobic) are available. Here, to elucidate the fate of PET-derived materials under anaerobic environments, a sludge-derived microbial community was cultured with bis(2-hydroxyethyl) terephthalate (BHET) as a model substrate for byproducts of PET degradation and dimethyl terephthalate (DMT) as a potential environmental pollutant discharged from the PET manufacturing process. Metagenome- and metabolome-informed microbiome analyses identified anaerobic BHET and DMT degradation pathways, uncultured organisms affiliated with Spirochaetota and Negativicutes predominant in the BHET-fed cultures, and *Methanomethylovorans* and Treponema_G predominant in the DMT-fed cultures. Metagenomic analyses newly identified three BHET-degrading and two DMT-degrading enzymes from the genomes of Spirochaeota. In addition, the Negativicutes in the BHET enrichment cultures possessed genes for acetogenically metabolizing EG and/or ethanol. Overall, this study successfully established anaerobic BHET- and DMT-degrading microbial consortia and newly proposed these degradation mechanisms under anaerobic conditions. This study indicated that the cultivation, microbiome, and metabolome analyses can be powerful tools for elucidating consortia capable of degrading plastics-associated waste compounds and the relevant metabolic mechanisms.

Keywords: *Polyethylene terephthalate (PET), bis(2-hydroxyethyl) terephthalate (BHET), dimethyl terephthalate (DMT), Spirochaeota, esterase, anaerobic biodegradation*

List of abbreviations

BHET: bis(2-hydroxyethyl) terephthalate

DMT: dimethyl terephthalate

PET: polyethylene terephthalate

PTA: purified terephthalic acid

EG: ethylene glycol

WWTPs: wastewater treatment plants

TA: terephthalic acid

MHET: mono-(2-hydroxyethyl) terephthalate

UASB: upflow anaerobic sludge blanket

MMT: monomethyl terephthalate

COD: chemical oxygen demand

BES: 2-bromoethanesulfonic acid

BC_A: autoclaved BHET medium

BC_U: unautoclaved BHET medium

$BC_{U\text{-}BES}$: unautoclaved BHET medium with BES

DC_A: autoclaved DMT medium

DC_U: unautoclaved DMT medium

$DC_{A\text{-}BES}$: autoclaved DMT medium with BES

TSP: 3-(trimethylsilyl)propionic acid-d 4 sodium salt

OTU: operational taxonomic unit

AhdE: bifunctional acetaldehyde/ethanol dehydrogenase

AldH: aldehyde dehydrogenase

Adh: alcohol dehydrogenase

Pta: phosphotransacetylase

AckA: Acetate kinase

BMC: bacterial microcompartments

1. Introduction

Polyethylene terephthalate (PET) was developed approximately 80 years ago and is now widely used worldwide, especially in production of PET bottles [1,2]. PET accounts for approximately 10% of total plastic production, with 33 million tons manufactured in 2015 [3–5]. PET is produced by polymerizing ethylene glycol (EG) with purified terephthalic acid (PTA) or dimethyl terephthalate (DMT) derived from petroleum resources [2]. In recent years, the release and accumulation of plastics waste on Earth has attracted global concern [2,5]. Plastics released into the environment can be fragmented to micro- and nano-plastics through abiotic/biotic transformation (*e.g.*, UV radiation and microbial degradation) [6], leading to ingestion by and harm towards aquatic and terrestrial animals. Therefore, the better understanding of the fate of released plastics is needed to prevent natural environments. With the recent attention of anaerobic digestion process treating wasted activated sludge discharged from wastewater treatment plants (WWTPs) as a major source of microplastic pollution [7], the fate of micro-plastics in various waste-treating processes is being studied [7,8]; however, little information is available on the organisms and metabolisms behind anaerobic digestion of micro-plastics.

Biodegradation of PET, its trimers, dimers, monomers, and their feedstock, such as terephthalic acid (TA) and DMT have been extensively studied to assess the environmental impact and biotoxicity of PET production processes, PET waste, and their degradation byproducts [1,9]. PET hydrolases have been reported from thermophilic bacterial strains of the genera *Thermobifida*, *Saccharomonospora*, and *Streptomyces* and the mesophilic bacterial genus *Ideonella* [10,11]. It has been reported that thermophilic PET hydrolases show excellent degradation rates of PET from an engineering perspective [11]. Although PET is considered to be stable and safe, synthesis precursors (*e.g.*, phthalate esters and DMT) and

degradation byproducts (*e.g.*, PET trimers) are biotoxic [1,9,12,13]. Therefore, it is essential to clarify the fate of these precursors and byproducts in the environment.

Hydrolytic organisms and enzymes have been reported for degrading PET to bis(2-hydroxyethyl) terephthalate (BHET) and mono-(2-hydroxyethyl) terephthalate (MHET) via PETases/cutinates, BHET and MHET to TA and EG via MHETases, and DMT to TA via esterase DmtH [9,14–16]; however, these studies are limited to aerobic organisms. Hotspots of waste microplastics include habitats that can contain anoxic zones, such as landfills [4] and coastal and deep-sea sediments at high concentrations [5,17]. Organisms and enzymes involved in hydrolyzing PET and DMT under anaerobic conditions and, thus, the fate of such material in natural and engineered environments remain largely unknown. Until now, information on the biodegradation of PET-related materials under anaerobic conditions has been limited to detection of DMT degradation [18], phthalate isomer-degrading syntrophic degraders (*i.e.*, *Pelotomaculum* [19] and *Syntrophorhabdus* [20]), and an anaerobe, *Clostridium thermocellum*, synthetically equipped with a known PET-degrading cutinase [21]. Understanding of the biodegradation of PET-related materials under anaerobic condition would be useful for elucidation of the fate of those materials in the environments and development cost-effective anaerobic treatment biotechnology (*e.g.*, energy recovery as methane gas and no requirement of oxygen supply).

Here, to obtain insight into the anaerobic biodegradation of PET hydrolysis byproducts and precursors, BHET- and DMT-degrading microbial consortia were activated and enriched by feeding sludge derived from an anaerobic bioreactor treating synthetic TA and DMT manufacturing wastewater [22] with BHET and DMT, respectively. Microbiome analyses employing 16S rRNA gene amplicon and shotgun sequence-based metagenomics and ^{1}H NMR-based metabolomics were performed to identify the anaerobic microorganisms driving BHET and DMT degradation.

2. Materials and Methods

2.1 Enrichment culture

Granular sludge samples taken from a lab-scale UASB reactor treating purified TA and DMT manufacturing synthetic wastewater under 81% chemical oxygen demand (COD) removal efficiency (organic loading rate: 1.0 kgCOD m^{-3} day^{-1}) [22] were used as seed sludge for the enrichment cultures. The basal medium was prepared according to a previous study [23]. All enrichment cultures were performed at 37 °C in 50-mL serum vials sealed with tight fitting butyl rubber stopper and aluminum crimp containing 20 mL of medium. The medium and atmosphere were flushed with N_2/CO_2 (80:20, v/v) gas at 0.1 MPa for 5 min. For transfer and sampling from the medium, 1 mL sterile plastic syringe was used. The BHET and DMT concentrations used for the enrichment cultures were 3.6 $g \cdot L^{-1}$. BHET enrichment cultures were prepared by the following three conditions: 1) autoclaved BHET medium prior to inoculation (BC_A); 2) unautoclaved BHET medium (BC_U); and 3) unautoclaved BHET medium with 5 mM 2-bromoethanesulfonic acid (BES) as a methanogenesis inhibitor ($BC_{U\text{-}BES}$) (transferred from the 10th enrichment culture in BC_U (BC_{U10})). DMT enrichment cultures were prepared by three conditions as follows: 1) autoclaved DMT medium prior to inoculation (DC_A); 2) unautoclaved DMT medium (DC_U) (transferred from the 8th A-DMT enrichment culture); and 3) autoclaved DMT medium with 5 mM BES ($DC_{A\text{-}BES}$) (transferred from the 8th enrichment culture in DC_A (DC_{8A})). BC_A and DC_A media were autoclaved at 121 °C for 20 min. The transfer volume of enrichment cultures into fresh medium was 10% (v/v). The enrichment cultures were routinely examined by a microscope equipped with a phase-contrast apparatus (BX-53, Olympus, Japan). The 1st, 2nd,7th, and 20th BC_U (BC_{1U}, BC_{2U}, BC_{7U}, and BC_{20U}), the BC_{1A} and BC_{7A} , and the $BC_{12U\text{-}BES}$, the 1st and 7–9th A-DMT (DC_{1A}, DC_{7A}, DC_{8A}, and DC_{9A}), DC_{1U} and DC_{4U} , and the $DC_{1A\text{-}BES}$ and $DC_{3A\text{-}BES}$ were

collected for DNA extraction. Two milliliters of the media of BC_{20U} , the $BC_{12U\text{-}BES}$, the 9th DC_{9A} , the DC_{1U} , and the $DC_{1A\text{-}BES}$ were used for ^{1}H NMR analysis. In addition, autoclaved or unautoclaved basal media were prepared with 3.6 $g \cdot L^{-1}$ BHET, 3.6 $g \cdot L^{-1}$ DMT, 3.6 $g \cdot L^{-1}$ MMT, 5 mM BES, or 0.1–10 mM TA for standard ^{1}H NMR analysis. Sampling days for each experiment were summarized in Table S1.

2.2 Analytical methods

Gas production volumes from the enrichment culture were determined using a 10–50 mL glass syringe at 37 °C. Before gas sampling, the butyl rubber stopper of the serum vial containing the medium was sterilized by 70% ethanol (v/v) and flame. The biogas components (CH_4, CO_2, N_2, and H_2) were determined by gas chromatography (Shimadzu, GC-8A, Japan) with a thermal conductivity detector fitted with a SHINCARBON-ST 50/80 stainless steel column 4.0 m × 3.0 mm (ID). The temperatures of the injection port/detector and the column were 150 and 130 °C, respectively.

Substrate degradation and intermediate production were analyzed by ^{1}H NMR spectra with a Bruker 600 MHz AVANCE III spectrometer (Bruker, Rheinstetten, Germany) operating at a proton frequency of 600.13 MHz and TopSpin 3.0 software (Bruker, Rheinstetten, Germany). Some of the cultures and liquid media were cryopreserved in 1.5-ml microtubes at -20 °C. On the day of the measurement, they were thawed at room temperature and centrifuged at 15,000 rpm (20,600 × g) at 2 °C for 1 min. Five hundred and forty μL of each supernatant and 60 μL phosphate-buffer stock solution were mixed to obtain NMR samples containing 50 mM NaP, 0.5 mM 3-(trimethylsilyl)propionic acid-d 4 sodium salt (TSP), 0.004% NaN_3 and 10% D_2O. They were centrifuged in 1.5-mL microtubes at 15,000 rpm (20,600 × g) at 2 °C for 1 min again, and 550 μL of the supernatants was transferred to a 5-mm NMR tube (Shigemi, Hachioji, Japan). ^{1}H NMR spectra were recorded at a sample

temperature of 298 K. All NMR spectral measurements were accumulated for 128 scans of 32,768 data points with 12 ppm spectral width and 2.27 s acquisition time. To delete the water peak and maximize the receiver gain, a *noesy1d* presaturation pulse sequence was employed with a low-power selective pulse at the water frequency. The recycle delay [D1 (Bruker notated)] was 2.7 s, and the mixing time [D8 (Bruker notated)] was 0.1 s. A 90° pulse length was automatically calculated at each sample analysis. All raw spectra were manually corrected for phase and baseline distortions and referenced to the TSP resonance at δ=0.0 ppm using TopSpin 4.1 software (Bruker, Rheinstetten, Germany). By referring to the peak area value of TSP as an internal standard, the spectra were normalized, and the relative integrated intensities of peaks due to the substrates and intermediates were calculated. Their concentrations were semiquantified by considering TSP concentration in the sample tube (0.5 mM), proton number of the object materials and TSP (H=9), and 90% dilution of original samples by the phosphate buffer.

2.3 DNA extraction, PCR amplification, and 16S rRNA gene sequence analysis

DNA extraction was performed using a FastDNA Spin Kit for Soil (MP Biomedicals, Santa Ana, California, USA) according to the manufacturer's protocol. The quality of extracted DNA was checked by electrophoresis (135 V, 20 min). DNA concentration was measured using Qubit 3.0 Fluorometer (Invitrogen, Carlsbad, CA, USA) assay with Qubit dsDNA BR assay kit (Invitrogen). The prokaryotic 16S rRNA genes were amplified using Univ515F–Univ909R [24] according to previous studies [22, 25]. The PCR reaction (20 μL) was carried out using a thermal cycler (TP600, Takara Bio, Shiga, Japan) with 1 ng template DNA, 0.5 μM forward and reverse primers, and 10 μL of Premix Ex Taq Hot Start Version (Takara Bio). The PCR cycle numbers were 25. The PCR products were purified using a

QIAquick PCR purification kit (Qiagen, Valencia, CA, USA). The sequence analysis of the purified 16S rRNA genes was performed by the MiSeq Reagent kit v3 and MiSeq system (Illumina, San Diego, CA, USA). Raw 16S rRNA gene sequences were treated by QIIME 2 ver. 2021.4 [26]. Quality trimming, primer sequence removal, paired-end assembly, and chimera checks were performed using DADA2 [27]. The observed high-quality 16S rRNA gene sequences were clustered by ≥97% similarity to operational taxonomic units (OTUs) using vsearch software [28]. Taxonomies of the OTUs were classified using classify-sklearn retained on the SILVA database version 138 [29].

2.4 Shotgun metagenomic sequence analysis

The DNA samples extracted from the 1st, 2nd, and 7th BHET enrichment cultures and the 7th DMT enrichment cultures were prepared with the ThruPLEX DNA-Seq Kit (Clontech, USA) with a library 200 length ranging between 273–418 bp. The prepared libraries were sequenced on a NovaSeq6000 (Illumina). The generated raw reads were trimmed using Trimmomatic 0.39 (SLIDINGWINDOW: 6:30 MINLEN: 100) [30]. De novo assembly was performed using Megahit v1.2.9 (--k-min 27 --k-max 141 --k-step 12) [31]. Coassembly of the BC_{1U}, BC_{2U}, and BC_{7U} enrichment cultures was performed to obtain good coverage of the contigs. The assembled contigs of short length (< 2,500 bp) were removed before binning treatment. Binning was performed using Metabat2 version 2.2.7 [32], MaxBin2 version 2.15 (-markerset 40) [33], MyCC (MyCC_2017.ova) [34], and Vamb version 3.0.3 [35] with default parameters. To obtain the high-quality metagenomic bins, obtained bins from the multiple binning results were refined using Das Tool version 1.1.2 (--score_threshold 0.5 --duplicate_penalty 0.6 --megabin_penalty 0.5) [36]. In the final step, the dereplication and genomic quality were checked by dRep version 3.2.0 (-comp 70 -con 10) [37].

The relative abundance rate of the metagenomic bins was calculated based on the median coverage produced from Metabat2 pipelines (jgi_summarize_bam_contig_depths, default parameters). All bins were annotated through a combination of Prokka v1.14.6 [38] and manual annotation. For the annotation of BHET and DMT esterase, metagenomic bins were assigned using blastp version 2.6.0 to known PET and MHET hydrolases (NCBI sequence IDs: 4OYY_A, AAZ54920, AAZ54921, AB728484, ACY95991, ACY96861, ADH43200, ADM47605, ADV92525, ADV92526, ADV92527, ADV92528, AEV21261, AFA45122, CAH17554, BAI99230, BAK48590, CBY05529, GAP38373, 6QZ2_A, JN129499, JN129500, MK681857, and QDD67397) [11] and esterase DmtH (AZI71502) [9] at the thresholds of ≥25% amino acid identity, ≤1e-10 e-value, and ≥70% query cover per subject (qcovs). Methanogenesis metabolisms of metagenomic bins were assigned to *Methanobacterium* (taxon_oid: 2630968343, 2645727909, 2681813006, 2684622658, 2791355014, and 2913397459), *Methanolinea* (2507262043, 2775507284, and 2913416594), *Methanomassiliicoccus* (GCF_000308215.1 and GCF_000404225.1), *Methanomethylovorans* (2509601008), *Methanoregula* (2508501105), *Methanospirillum* (2606217615), and *Methanothrix* (2724679722) at the thresholds of ≥60% identity, ≤1e-20, and ≥70% qcovs. For the annotation of EG, ethanol and methanol degradation through acetogenic metabolism, predominant metagenomic bins were assigned to the genome of *Acetobacterium woodii* DSM1030 (GCA_000247605.1) at the threshold of < 1e-5 evalue. Furthermore, core genes of acetogenesis were automatically annotated using BlastKOALA [39] and DRAM software (--use_uniref option with default setting) [40]. Reference genomes with taxon_oid were obtained from the Joint Genome Institute (JGI) genome portal [41]. Putative BHET- and DMT-degrading proteins were aligned with known BHET/MHET-degrading enzymes [11] and reference esterase with DMT-degrading enzymes obtained from Cheng et al. [9], respectively. The alignment software mafft-linsi v7.480 (default parameters) was used [42].

Phylogenetic trees of BHET/MHET- and DMT-degrading proteins were constructed using iqtree2 version 2.1.2 (-B 1000) with automatically optimized substitution models of Blosum62+F+I+G4 and WAG+F+R4, respectively [43]. The taxonomic classification of the bins was estimated using GTDBtk v1.5.1 (GTDB release202; default parameters) [44].

2.5 Molecular modeling and docking simulation

Structural models were predicted using AlphaFold2, which is a newly developed neural network-based model [45]. The resulting predicted local distance difference test (pLDDT) value is above 89, indicating that the predictions can be considered highly accurate. For docking simulation between enzymes and ligands, hydrogen atoms and charges were added using the Docking prep tool in Chimera software version 1.15 [46]. Finally, molecular docking was performed using AutoDock Vina ver. 1.2.0 [47]. 2D docked poses were generated using the Maestro software ver. 13.0.137 (Schrödinger, LLC, NY).

2.6 Deposition of DNA sequence data

The raw sequence and binned metagenome data were deposited into the DDBJ Sequence Read Archive database (DRA013833).

3. Results and Discussion

3.1 Enrichment of BHET- and DMT-degrading consortia

For the enrichment of BHET- and DMT-hydrolyzing microorganisms, the cultures were sequentially transferred into fresh medium at 1–2-week intervals, and gas production and composition were monitored. In addition, to confirm the influence of abiotic hydrolysis and hydrogenotrophic methanogens, the enrichment cultures of BHET and DMT were transferred into fresh media with nonautoclaving/autoclaving treatments or addition of BES

as a methanogenesis inhibitor, respectively. Regarding the BHET enrichment cultures, hydrogen and methane gas production could not be confirmed from the enrichment culture in autoclaved BHET medium prior to inoculation (BC_A) throughout the culture period, while gas production was confirmed from the enrichment cultures using unautoclaved BHET cultures (BC_U) (Table 1). Hydrogen gas production was confirmed only from BC_{17U} (Table 1). In the $BC_{U\text{-}BES}$ transferred from the BC_{10U}, methane gas production was completely inhibited, and only hydrogen production occurred. The ^{1}H NMR analysis showed that 8.5 mM MHET and 0.5 mM TA or 6.4 mM MHET and 0.3 mM TA in BC_{20U} and $BC_{12U\text{-}BES}$ were produced from 11.0 or 10.6 mM BHET originally in basal medium (BC_U and $BC_{U\text{-}BES}$), respectively (Fig. 1A and Table 2). Despite MHET and TA being produced at similar amounts, a major difference in the byproducts of these cultures was accumulation of EG (8.2 mM), rather than acetate, in the absence of BES (Fig. 1B and Table 2), suggesting that methanogenesis heavily influence downstream degradation of BHET (*i.e.*, post-hydrolysis) in this microbial community. It has been reported that short-chain fatty acids accumulation occurred by shortened retention time for fermentation of waste activated sludge [48], so acetate production in the $BC_{12U\text{-}BES}$ may be related to the short incubation times (approximately 6.2 days for each cultivation). The reason for the lack of production of methane and hydrogen gases in BC_A was that BHET was mostly converted to MHET, EG, and TA in the original medium of BC_A (Fig. 1C and Table 2); therefore, the relatively short transfer period (1–2 weeks) may have prevented the growth of slow-growing syntrophs such as *Syntrophorhabdus* and *Pelotomaculum* (*e.g.*, 20 days as doubling time of *S. aromaticivorans*) [19,20,49], which can degrade TA and EG.

To identify which microorganisms were enriched in the BHET- and DMT-fed cultures, 16S rRNA-based microbial community structure analysis was performed (Fig. 2A and Table S2). The obtained results showed that the microbial communities significantly

differed between the enrichment cultures using BC_A and BC_U. For example, members of *Ralstonia* (BHET003, 37%), *Rhodococcus* (BHET005, 33%), and *Spirochaetaceae* (BHET002, 24%) predominated in BC_{7A}, while unclassified Negativicutes (BHET001, 85%), *Methanospirillum* (BHET013, 6.5%), unclassified Spirochaetaceae (BHET015, 3.2%), and unclassified Sporomusaceae (BHET004, 1.9%) were detected in BC_{7U}. Microscopic observation showed rod-shaped cells attached to the BHET crystals in the BC_{7U} (Fig. 3A), while almost no BHET-like crystals or microbial cells were observed in the BC_{7A} (data not shown). Furthermore, unclassified Negativicutes (BHET001) and unclassified Sporomusaceae (BHET004) accounted for 97% in the BC_{20U} (Fig. 2A). In the BC_{20U} and $BC_{12U\text{-}BES}$, there were no hydrogenotrophic and aceticlastic methanogens in the BHET enrichment cultures.

Table 1. Gas production volumes from the bis(2-hydroxyethyl) terephthalate (BHET) and dimethyl terephthalate (DMT) enrichment cultures

		Gas production volume (NmL)																			
		1st[h]	2nd	3rd	4th	5th	6th	7th	8th	9th	10th	11th	12th	13th	14th	15th	16th	17th	18th	19th	20th
BC_U[a]	Days[g]	8.1	11.9	8.1	7.9	8.0	10.0	6.9	9.0	6.9	8.0	6.8	8.9	6.8	6.9	6.9	4.0	8.0	3.9	8.9	7.0
	Total	11.0	4.4	4.8	5.7	5.3	1.0	4.0	7.1	4.0	5.1	2.2	5.5	6.0	2.8	1.9	3.5	3.9	1.9	1.8	2.3
	CH_4	2.6	0.9	0.5	0.2	0.3	0.7	0.6	0.8	0.6	0.7	0.3	0.4	N.D.[i]	0.3	0.5	N.D.	0.0	0.0	0.0	0.0
	H_2	0.0	0.0	0.5	0.5	0.7	0.0	0.0	0.0	0.0	0.0	0.1	0.0	N.D.	0.3	0.0	N.D.	0.9	0.5	0.8	0.5
BC_A[b]	Days	8.0	11.9	8.0	7.9	8.0	6.9	9.0	-[j]	-	-	-	-	-	-	-	-	-	-	-	-
	Total	8.4	5.7	2.6	4.0	3.1	1.3	2.2	-	-	-	-	-	-	-	-	-	-	-	-	-
	CH_4	1.6	0.1	0.0	0.0	0.0	0.0	0.0	-	-	-	-	-	-	-	-	-	-	-	-	-
	H_2	0.0	0.0	0.0	0.0	0.0	0.0	0.0	-	-	-	-	-	-	-	-	-	-	-	-	-
$BC_{U\text{-}BES}$[c]	Days	5.8	8.9	6.8	6.9	7.0	4.0	8.0	7.0	5.0	8.9	8.0	6.9	-	-	-	-	-	-	-	-
	Total	2.3	5.5	4.4	1.9	2.3	2.3	4.8	2.6	3.7	3.0	3.7	3.4	-	-	-	-	-	-	-	-
	CH_4	0.0	0.0	N.D.	0.0	0.0	N.D.	0.0	0.0	N.D.	0.0	0.0	0.0	-	-	-	-	-	-	-	-
	H_2	0.0	0.7	N.D.	0.7	0.7	N.D.	0.9	0.5	N.D.	0.8	0.5	1.6	-	-	-	-	-	-	-	-
DC_A[d]	Days	8.0	12.5	8.0	7.8	8.0	9.9	6.9	8.9	6.8	-	-	-	-	-	-	-	-	-	-	-
	Total	12.8	11.0	7.5	7.1	7.1	4.4	5.3	11.9	4.8	-	-	-	-	-	-	-	-	-	-	-
	CH_4	9.2	7.7	6.4	3.6	4.6	3.0	3.7	6.0	4.6	-	-	-	-	-	-	-	-	-	-	-
	H_2	0.0	0.0	0.0	0.0	0.0	0.0	0.0	0.0	0.0	-	-	-	-	-	-	-	-	-	-	-
DC_U[e]	Days	11.9	12.9	10.9	17.0	-	-	-	-	-	-	-	-	-	-	-	-	-	-	-	-
	Total	4.1	3.4	4.9	3.2	-	-	-	-	-	-	-	-	-	-	-	-	-	-	-	-
	CH_4	0.4	0.0	N.D.	N.D.	-	-	-	-	-	-	-	-	-	-	-	-	-	-	-	-
	H_2	0.0	0.0	N.D.	N.D.	-	-	-	-	-	-	-	-	-	-	-	-	-	-	-	-
$DC_{A\text{-}BES}$[f]	Days	11.7	12.9	10.9	-	-	-	-	-	-	-	-	-	-	-	-	-	-	-	-	-
	Total	4.2	4.2	5.8	-	-	-	-	-	-	-	-	-	-	-	-	-	-	-	-	-
	CH_4	0.0	0.0	N.D.	-	-	-	-	-	-	-	-	-	-	-	-	-	-	-	-	-
	H_2	0.0	0.0	N.D.	-	-	-	-	-	-	-	-	-	-	-	-	-	-	-	-	-

[a]Unautoclaved bis(2-hydroxyethyl) terephthalate (BHET)-amended medium

[b]Autoclaved BHET-amended medium

[c]Unautoclaved BHET-amended medium with 2-bromoethanesulfonic acid (BES)

[d]Autoclaved dimethyl terephthalate (DMT) medium

[e]Unautoclaved DMT medium

[f]Autoclaved DMT medium with BES

[g]Cultivation and transferring days

[h]Cultivation times

[i]Not determined

[j]No data

Table 2. Substrate and intermediate concentrations of enrichment cultures and basal media based on ^{1}H NMR analysis

	Substrates and intermediates concentration (mM)								
	BHET	MHET[g]	DMT	MMT[h]	Terephthalate	Ethylene glycol	Methanol	Acetate	Formate
BC_{20U}[a]	7.9	8.5	0.0	0.0	0.5	8.2	0.0	0.0	0.0
$BC_{12U\text{-}BES}$[b]	7.6	6.4	0.0	0.0	0.3	0.0	0.2	4.9	0.2
BC_{U}[c]	11.0	0.4	0.0	0.0	0.0	0.2	0.0	0.0	0.0
$BC_{U\text{-}BES}$	10.6	0.3	0.0	0.0	0.0	0.0	0.0	0.0	0.0
BC_{A}[d]	1.9	11.5	0.0	0.0	2.2	13.7	0.0	0.0	0.0
DC_{9A}[e]	0.0	0.0	0.2	12.0	2.6	0.0	11.0	0.0	0.0
DC_{1U}[f]	0.0	0.0	0.1	1.9	0.5	0.0	0.0	0.0	0.0
$DC_{1A\text{-}BES}$	0.0	0.0	0.1	12.1	2.6	0.0	11.1	0.0	0.0
DC_{A}	0.0	0.0	0.1	8.0	0.9	0.0	6.8	0.0	0.0
$DC_{A\text{-}BES}$	0.0	0.0	0.1	6.7	0.8	0.0	5.6	0.0	0.0
DC_{U}	0.0	0.0	0.1	0.0	0.0	0.0	0.0	0.0	0.0

[a]Enrichment culture in unautoclaved bis(2-hydroxyethyl) terephthalate (BHET)-amended medium after 20 transfers

[b]Enrichment culture in unautoclaved BHET-amended medium with 2-bromoethanesulfonic acid after 12 transfers

[c]Basal medium of unautoclaved BHET-amended medium

[d]Basal medium of autoclaved BHET-amended medium

[e]Enrichment culture in autoclaved dimethyl terephthalate (DMT)-amended medium after 9 transfers

[f]Enrichment culture in unautoclaved DMT-amended medium after 1 transfer

[g]Mono(2-hydroxyethyl) terephthalate

[h]Monomethyl terephthalate

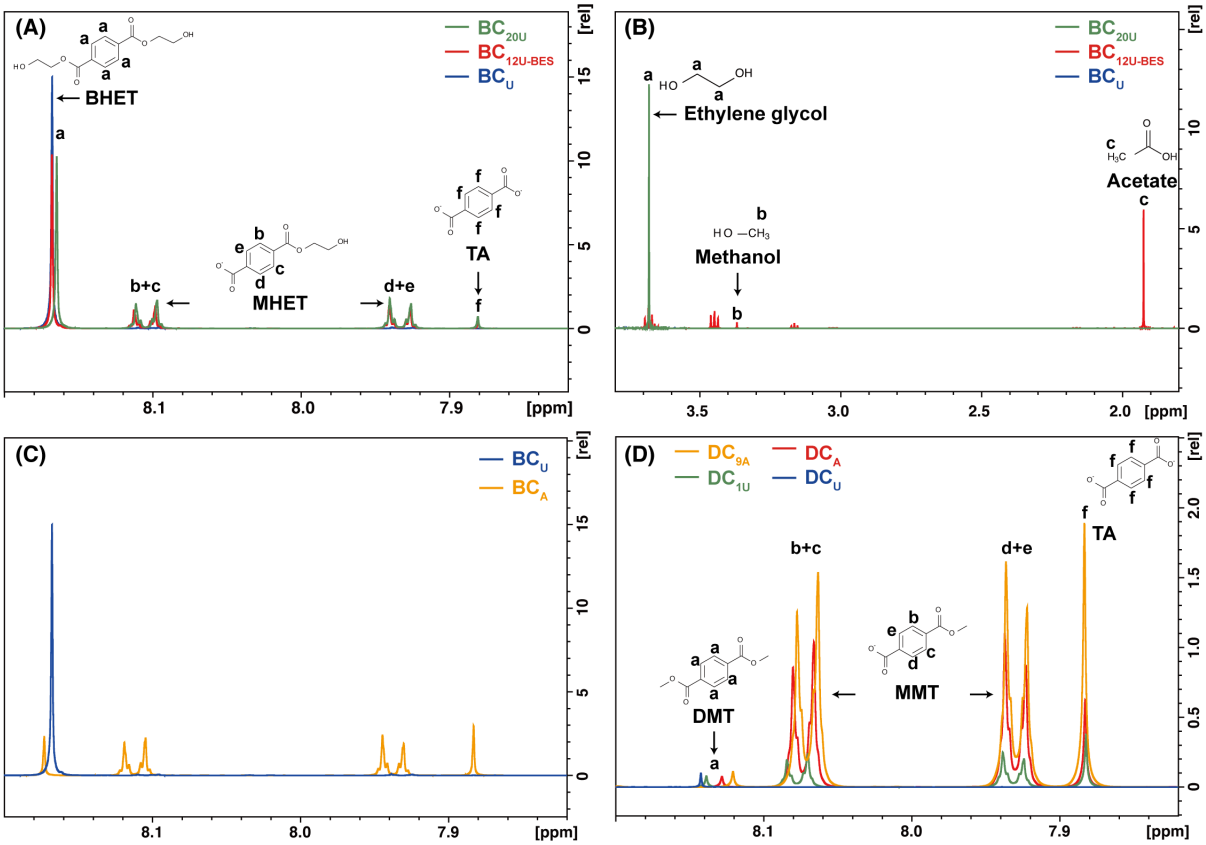

Fig. 1 ^{1}H NMR spectrum from (A) and (B) enrichment culture in unautoclaved bis(2-hydroxyethyl) terephthalate-amended medium after 20 transfers (BC_{20U}), BC_{12U} with 2-bromoethanesulfonic acid (BES) ($BC_{12U\text{-}BES}$), basal medium of unautoclaved BHET cultures (BC_U), (C) BC_U and autoclaved basal medium amended with BHET (BC_A), and (D) enrichment culture in autoclaved dimethyl terephthalate-amended medium after 9 transfers (DC_{9A}), DC_{1U}, DC_A, and DC_U; (A) and (C) spectra of BHET, mono(2-hydroxyethyl) terephthalate (MHET), and terephthalate (TA); (B) spectra of ethylene glycol, methanol, and acetate; (D) spectra of DMT, monomethyl terephthalate (MMT), and TA.

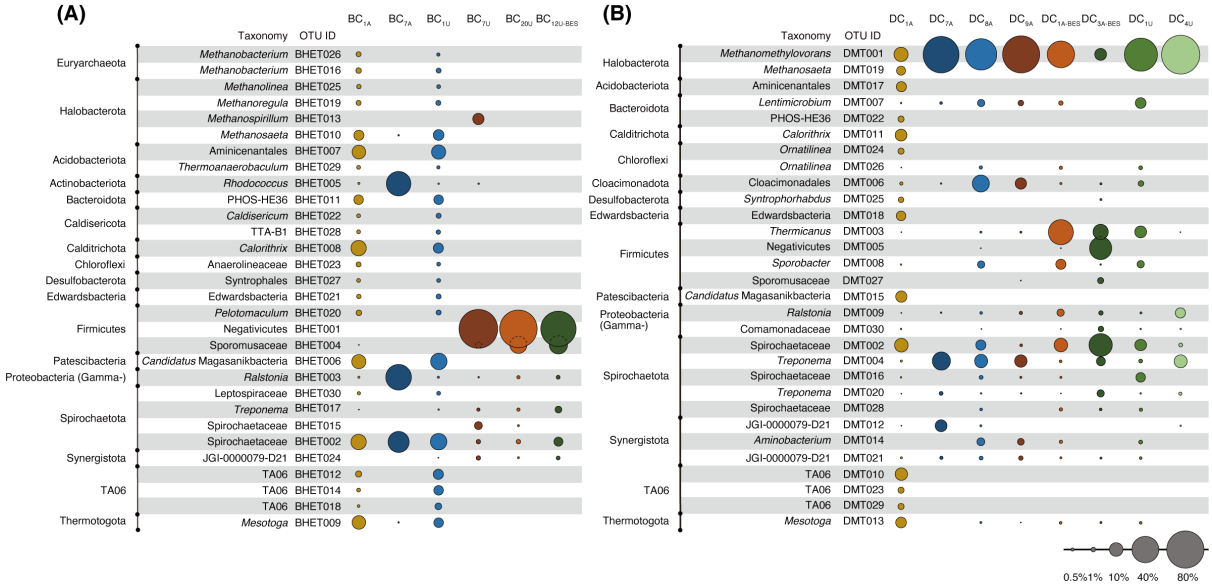

Fig. 2 Abundance of predominant operational taxonomic units (OTUs) in (A) the enrichment cultures of autoclaved/unautoclaved bis(2-hydroxyethyl) terephthalate (BHET) media and the (B) enrichment cultures of autoclaved/unautoclaved dimethyl terephthalate (DMT) media using bubble plots. Circle size corresponds to abundance rate, as shown at the bottom of the figure.

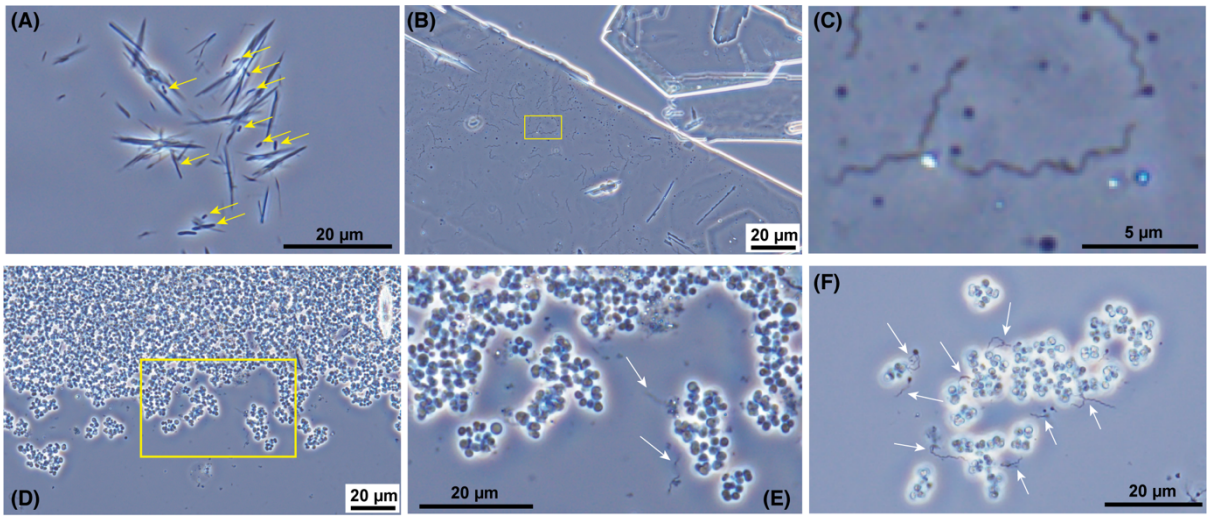

Fig. 3 Phase-contrast micrographs of (A) enrichment culture in unautoclaved bis(2-hydroxyethyl) terephthalate-amended medium after 7 transfers (BC_{7U}) and (B)–(F) enrichment culture in autoclaved dimethyl terephthalate-amended medium (DC_{7A}) on cultivation days 11. Yellow arrows indicate attached microbial cells on the BHET crystals. Yellow squares indicate high-magnification parts of (C) and (E). White arrows indicate Spirochaeota-like cells attached to Methanomethylovorans-like cells.

In the DMT enrichment cultures, methane gas production was observed in the cultures of DC_A throughout the period, and no hydrogen gas was detected (Table 1). For the DC_{2U}–DC_{4U}, the methane and hydrogen gas volumes were below the detection limit of the gas chromatography. Methane production was completely inhibited in the enrichment cultures of $DC_{A\text{-}BES}$. NMR analysis showed that 12.0 mM, 1.9 mM, and 12.1 mM MMT, 2.6 mM, 0.5 mM, and 2.6 mM TA, and 11.0 mM, 0 mM, and 11.1 mM methanol were detected in the DC_{9A}, DC_{1U}, and $DC_{1A\text{-}BES}$ after cultivation, respectively. The concentration of DMT did not change before and after cultivation (0.09-0.14 mM) because of its low solubility (19 $mg \cdot L^{-1}$) and the addition of DMT at an amount two orders higher than this solubility (Fig. 1D and Table 2). In the basal medium of DC_A, 8.0 mM MMT, 0.9 mM TA, and 6.8 mM methanol were produced by autoclaving treatment, which is the reason for the high concentrations of

MMT and methanol after cultivation. In the basal DC_U, MMT and TA were only detected after cultivation (Fig. 1D and Table 2), indicating biological degradation of DMT. Methanol was not detected after cultivation in the DC_{1U} because methanol produced by hydrolysis of DMT was likely rapidly utilized by microorganisms in the culture. Furthermore, there was no significant change in the concentration of metabolites in the presence or absence of BES, suggesting that BES had little effect on the degradation of DMT.

Amplicon sequencing using the 16S rRNA gene as a target showed that these DMT enrichment cultures were dominated by a methanol-utilizing methanogen *Methanomethylovorans* (DMT001, 73%), *Treponema* (DMT004, 18%), and uncultured Synergistaceae JGI-0000079-D21 (DMT012, 6.9%) (Fig. 2B and Table S3). Microscopic observations revealed that Spirochaeota-like cells were attached to the DMT-like crystals, and flocs of *Methanomethylovorans*-like coccoid cells were abundant in the enrichment cultures (Figs. 3B-3E), suggesting that *Treponema* (DMT004) may degrade DMT and the byproduct methanol can be converted to methane gas by *Methanomethylovorans* (DMT001). Subsequently, the abundance of JGI-0000079-D21 (DMT012) decreased, and that of Cloacimonadales (DMT006) increased in the enrichment cultures after 8 and 9 transfers (DC_{8A} and DC_{9A}) (Fig. 2B and Table S3). In the $DC_{1A\text{-}BES}$, the abundance of *Methanomethylovorans* (DMT001) decreased to 40% (1st transfer) and 7.4% (3rd), and unclassified Negativicutes (DMT005) and Spirochaetaceae OTUs (DMT002, DMT004, and DMT020) increased. In addition, the predominant OTUs of DC_U and DC_A were *Methanomethylovorans* (DMT001) and Spirochaetaceae OTUs (DMT002 and DMT004) regardless of the autoclaving treatment.

3.2 BHET degradation metabolism

Shotgun metagenomic analysis of the BC_{1U}, BC_{2U}, and BC_{7U} was performed to elucidate the metabolic functions of microorganisms involved in BHET degradation. The uncultured phylogenetic groups, such as Patescibacteria (BHET40.001) and WOR-3 (BHET_531 and BHET40.002), were predominant in the early enrichment cultures, whereas in after the 7 transfers, metagenomic bins of the Firmicutes_C (BHET.Bin.209 and BHET40.249), Halobacteriota (BHET.Bin.162), and Spirochaetota (Cluster.64, BHET.Bin.69, BHET40.136, and BHET_244_sub) were enriched (Fig. 4A). In particular, BHET.Bin.209 belonging to the uncultured group UBA11029 of the class Negativicutes accounted for 88% of the community and was the most abundant metagenomic bin in the BC_{7U}. The results of 16S rRNA gene analysis were similar to those obtained by metagenomic analysis (Fig. 2A), indicating that the genomes of the predominant microorganisms in the BC_{7U} were correctly recovered in this study.

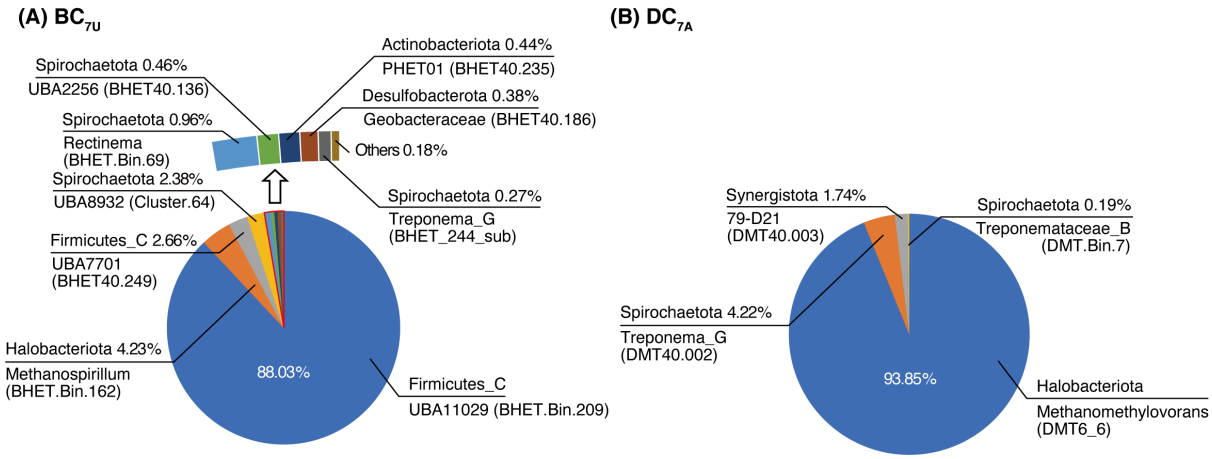

Fig. 4 Proportions of observed metagenomic bins from (A) the enrichment culture in unautoclaved bis(2-hydroxyethyl) terephthalate (BHET)-amended medium (BC_{7U}) and the (B) enrichment culture in autoclaved dimethyl terephthalate (DMT)-amended medium (DC_{7A}).

To identify the BHET degradation pathway, a blastp-based homology search with known PET degradation-related genes was performed for metagenomic bins collected from the BC_{7U}. The obtained results showed that Treponematales (Cluster.64 and BHET40.136) and Treponema_G (BHET_244) belonging to the phylum Spirochaeota possess genes that showed 36% (Cluster.64_00965, 6.9e-64), 34% (BHET40.136_00755, 7.1e-59) and 29% (BHET_244_sub_02548, 3.4e-49) homology with p-nitrobenzylesterase of *Bacillus subtilis* 4P3-11(BsEstB, ADH43200.1) [50], respectively (Table S7). These genes conserved the active sites, including the GxSxG motif and catalytic triad (Ser, His, and Glu), as in known PET-degrading enzymes (Table S8). The three identified putative BHET-degrading enzymes were phylogenetically analyzed together with the known PET- and MHET-degrading enzymes (Fig. 5A). As a result, these genes were placed with BsEstB (ADH43200.1) in *B. subtilis* and cutinase (4OYY_tr) in *Humicola*, which were different clades from PETase and cutinase in *Thermobifida*, *Thermomonospora*, and *Ideonella*. To further investigate the interaction of these enzymes with BHET and MHET, the molecular modeling of Cluster.64_00965, BHET40.136_00755, and BHET_244_sub_02548 was performed, which showed ≥28% homology (<1e-48 as e-value) to BsEstB, and the docking simulation of these predicted structures with substrates. The obtained results showed that these enzymes have the binding pocket to bind BHET, which could be bound to the substrate with hydrogen bonding, π-π stacking interactions, and hydrophobic interactions. Furthermore, the three amino acid residues comprising the catalytic triad (Ser-217, His-432, Glu-353 for Cluster.64_00965, Ser-232, His-451, Glu-367 for BHET40.136_00755, Ser-200, His-411, Glu-323 for BHET_244_sub_02548) are close to each other in the predicted three-dimensional structures, and the active Ser in these is located on the surface of the binding pocket (Fig. 6A). Thus, these three enzymes are capable of degrading BHET. Interestingly, even during MHET binding, the active Ser is located near the ester bond of MHET (Fig. 6A). *B. subtilis*-derived

BsEstB, which has a catalytic triad as well as Spirochaeota-derived enzymes, is known to degrade both BHET and MHET [50]. Therefore, these enzymes may degrade not only BHET but also MHET.

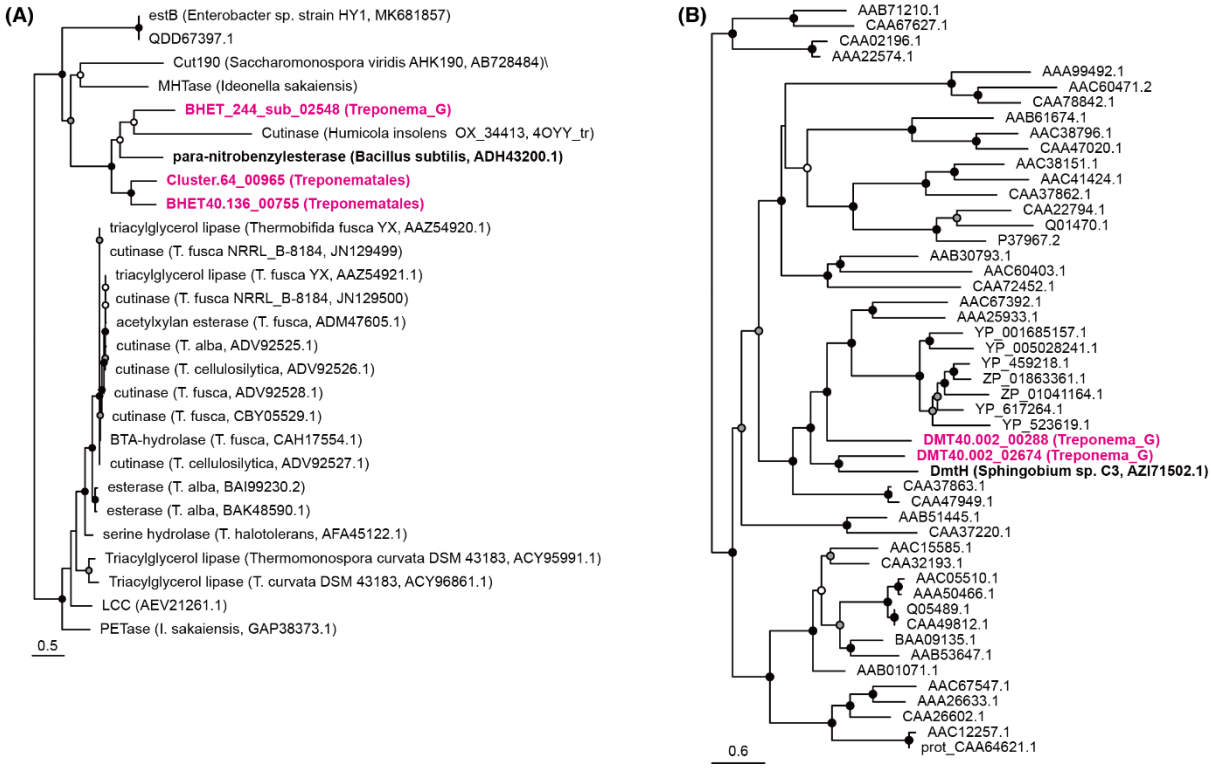

Fig. 5 Phylogenetic tree calculated by the maximum likelihood method showing the affiliations of (A) PET hydrolase, including cutinase, PETase, MHETase, lipase, and BHET hydrolases, and (B) DMT hydrolase (DmtH) with other esterases and lipases. Highlighted pink colors indicate the putative BHET hydrolases and DMT hydrolase. The black, gray, and white circles indicate the ultrafast bootstrap (1000 replicates)-supported probabilities at >90%, >70%, and >50%, respectively.

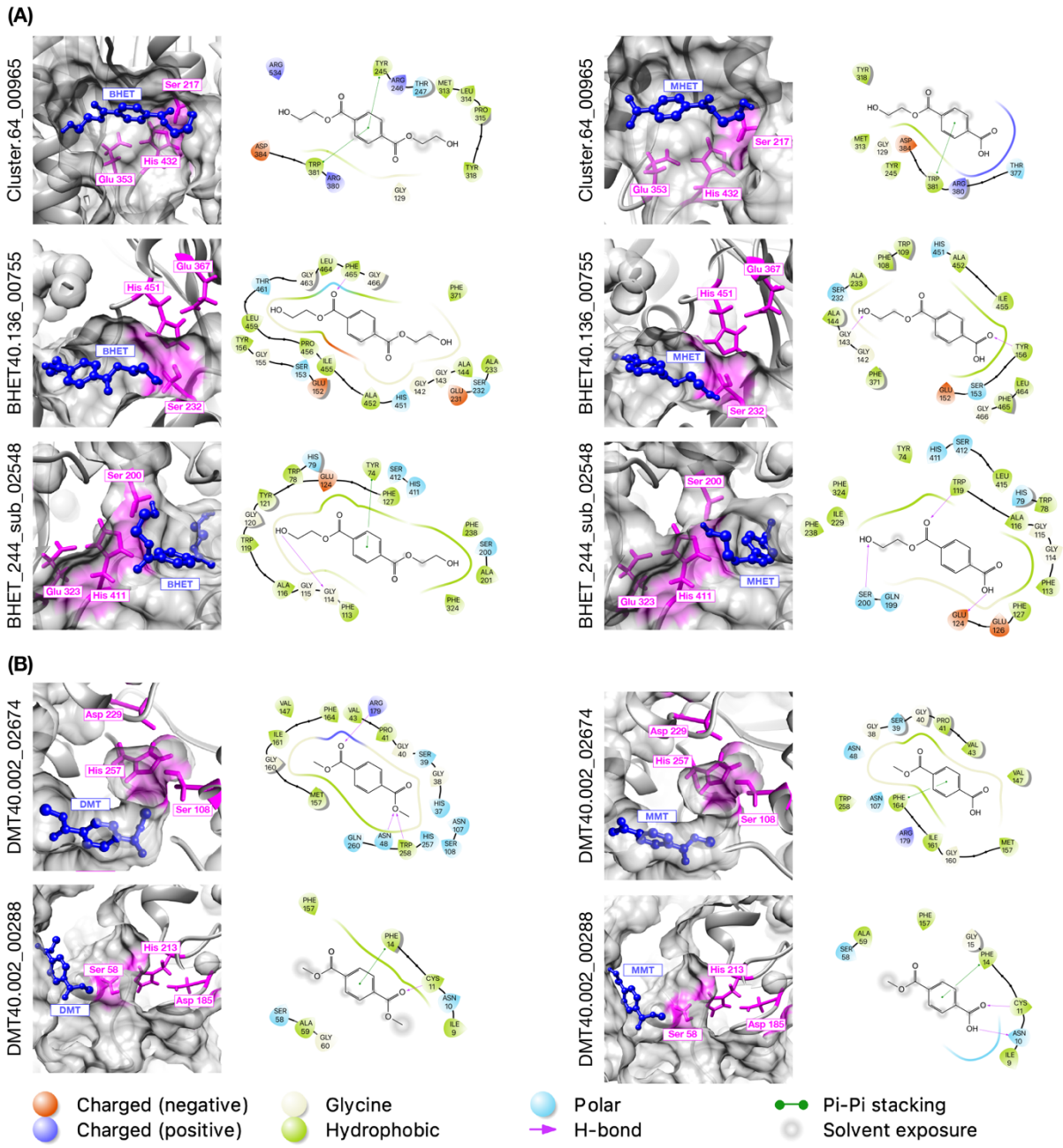

Fig. 6 3D docking models and 2D interaction diagrams between the predicted structures of enzymes and substrates. (A) PET hydrolase docked with BHET or MHET. (B) DMT hydrolase docked with DMT or MMT. The catalytic triad (Ser, His, Glu/Asp) and substrates in the docking model are highlighted in magenta and blue, respectively.

Given the results of enrichment cultures and ^{1}H NMR analysis, it is predicted that MHET and EG were formed after hydrolysis of BHET and further degradation of these

compounds yielded TA and ethanol. Furthermore, ethanol could be converted to acetate by acetogen (Table 2 and Fig. 1A). To further clarify the microorganisms relevant to BHET metabolism and their roles in the BHET enrichment cultures, metabolic reconstruction was performed for the predominant metagenomic bins. Anaerobic degradation of EG is known to proceed through syntrophic degradation [51] or acetogenesis [52]. As BHET degradation occurred when BES was added as a methanogenesis inhibitor (Table 2) and methanogens were not detected in BC_{20U} (Fig. 2B), it was assumed that EG was degraded acetogenically. Therefore, a blastp amino acid sequence homology search was performed against the genome sequence of an acetogenic EG degrader, *A. woodii*. The obtained results showed that while predominant populations predicted to possess BHET-hydrolyzes enzymes (*i.e.*, Treponematales Cluster.64, BHET40.136, and BHET_244_sub) lacked genes involved in EG degradation (specifically pduCDE and pduP), one Sporomusales population (BHET40.249) possessed genes homologous to those for EG degradation in *A. woodii* (Fig. 7 and Table S11) [53], indicating that this organism may be responsible for EG utilization.

Acetaldehyde and ethanol produced via EG degradation are known to be further decomposed by a bifunctional acetaldehyde/ethanol dehydrogenase (AdhE) or a combination of aldehyde dehydrogenase (AldH) and alcohol dehydrogenase (Adh). Then, the produced acetyl-CoA is converted to acetate via phosphotransacetylase (Pta) and acetate kinase (AckA) [52, 54]. The most abundant metagenomic bin, Negativicutes (BHET.Bin.209), possesses 11 homologs of AhdE and Adh (Table S13) and most of the core genes of the Wood-Ljungdahl pathway (Table 3). This suggests that the microorganism obtains energy from ethanol via acetogenesis. Sporomusales (BHET40.249) also possessed core genes other than MetV, acsE, and CODH/ACS, suggesting that BHET40.249 may grow by ethanol-mediated acetogenesis. Therefore, although the detailed mechanisms remain unknown, it is suggested that acetate detected in the $BC_{12U\text{-}BES}$ was produced from Negativicutes (BHET.Bin.209) and

Sporomusales (BHET40.249). Further investigation is required to be clarified whether the lack of some core genes of acetogenesis is due to genomic incompleteness by reconstructing the complete genome. Treponematales (Cluster.64), Treponematales (BHET40.136), and Treponema_G (BHET_244_sub), which possess putative BHET-degrading enzymes, have homologs of AdhE, Adh, AldH, Phosphotransacetylase (Pta) and Acetate kinase (AckA) (Table S13), but lack most of the core genes for acetogenesis (Table 3). On the other hand, these bins have multiple glycoside hydrolases, peptides, and amino acid transporters, such as branched-chain amino acid transport systems, oligopeptide transport systems, and sugar transport systems (Tables S15 and S16). Although further investigation is necessary, it is possible that the Spirochaeota lineages likely obtain nutrients by acquiring substrates such as metabolites of predominant microorganisms such as Negativicutes lineages that metabolize BHET degradation products.

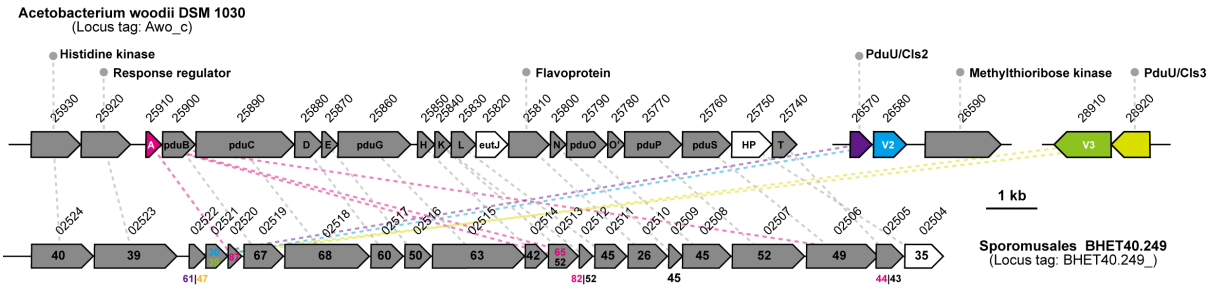

Fig. 7 Gene clusters involved in ethylene glycol (EG) degradation in *Acetobacterium woodii* DSM 1030 and Sporomusales (BHET40.249). Numbers in gene boxes indicate the amino acid sequence identity (%) and the corresponding gene of *A. woodii* DSM 1030. Abbreviations: A, pduA; E, pduE; H, pduH; K, pduK; M, pduM; N, pduN; T, pduT; U, pduU; V, pduV; V2, pduV2; V3, pduV3; and HP: hypothetical protein. Gene labels of the gene clusters follow Chowdhury et al., 2020 [53]. pduA, pduB, pduK, pduN, and pduT are bacterial microcompartments (BMC). pduCDE and pduG are the propanediol dehydratase and dehydratase activation proteins, respectively. pduL, pduO, pduP, and pduS are phosphate

propanoyltransferase, ATP-cobalamin adenosyltransferase, CoA-dependent aldehyde-dehydrogenase, and cobalamin reductase, respectively. The pduCDE and pduP proteins are putative EG dehydration enzymes (from EG to acetaldehyde) according to Trifunović et al., 2016 [52].

Table 3. Locus tags of predominant Negativicutes and Spirochaeota bins for genes encoding the methyl and carbonyl branches in the Wood-Ljungdahl pathway and aldehyde:ferredoxin oxidoreductase.

Gene name	abbr.	Negativicutes BHET.Bin.209	Sporomusales BHET40.249	Treponematales Cluster.64	Treponematales BHET40.136	Treponema_G BHET_244_sub	Treponema_G DMT40.002
formate dehydrogenase (FDH)	fdhF	BHET.Bin.209_00948	BHET40.249_01626 BHET40.249_01627 BHET40.249_03267 BHET40.249_03268				
	fdhD	BHET.Bin.209_02432					
formyl-tetrahydrofolate synthase (FHS)	fhs	BHET.Bin.209_00240	BHET40.249_01056 BHET40.249_01130 BHET40.249_01606				
formyl-cyclohydrolase (FCH)	fchA		BHET40.249_01057 BHET40.249_01129 BHET40.249_03966				
methylene-THF dehydrogenase (MDH)	folD	BHET.Bin.209_00241	BHET40.249_01607	Cluster.64_00474	BHET40.136_01630	BHET_244_sub_02185	DMT40.002_00487
methylene-THF reductase (MR)	metV						
	metF	BHET.Bin.209_00304 BHET.Bin.209_02278	BHET40.249_03495				
methyltransferase (MT)	acsE						
carbon monoxide dehydrogenase/ acetyl-CoA synthase (ACS/CODH)	acsA	BHET.Bin.209_01373 BHET.Bin.209_01391					
	acsB	BHET.Bin.209_02751					
	acsC						
	acsD						
	acsF						
	cooC	BHET.Bin.209_02750					
phosphotrans-acetylase (PTA)	pta	BHET.Bin.209_00235	BHET40.249_00150 BHET40.249_00617 BHET40.249_02416 BHET40.249_02511	Cluster.64_00248	BHET40.136_00055 BHET40.136_01578		
acetate kinase (ACK)	ack	BHET.Bin.209_00267 BHET.Bin.209_00268	BHET40.249_00320	Cluster.64_01463	BHET40.136_01673	BHET_244_sub_00298 BHET_244_sub_02281	DMT40.002_00745 DMT40.002_01913
aldehyde:ferredoxin oxidoreductase (AOR)	aor	BHET.Bin.209_00509 BHET.Bin.209_01414 BHET.Bin.209_01417 BHET.Bin.209_01640 BHET.Bin.209_02613 BHET.Bin.209_02635 BHET.Bin.209_02884	BHET40.249_01625 BHET40.249_02244	Cluster.64_01157 Cluster.64_01185 Cluster.64_01404	BHET40.136_01727		

3.3 DMT degradation metabolism

For DMT enrichment cultures, metagenomic analysis of the DC_{7A} culture was performed. Four metagenomic bins were recovered, which belong to *Methanomethylovorans* (DMT6_6, 93.9%), Treponema_G (DMT40.002, 4.2%), Synergistales (DMT40.003, 1.7%), and Treponemataceae_B (DMT.Bin.7, 0.2%) (Fig. 4B). The phylogeny and abundance of the recovered metagenomic bins reflect the results of 16S rRNA gene analysis and microscopic observations (Figs. 2B, 3B, and 3C and Table S3). The genus Treponema_G (DMT40.002) showed 98.9% ANI with BHET_244_sub recovered from the BHET enrichment cultures (Table S6), suggesting that the genomes may be from closely related species/strains.

To identify novel DMT-degrading enzymes, a blastp-based homology search was performed against the known esterase DmtH [9]. The obtained results showed that the metagenomic bin DMT40.002 belonging to Treponema_G possessed esterases with 31.6% (DMT40.002_02674, 8.5e-39) and 26.6% (DMT40.002_00288, 5.7e-12) homology (Table S7). These genes also conserved their active sites (Ser, Glu, and His) and the GxSxG motif (Table S10). Furthermore, phylogenetic analysis of these identified genes showed that the esterase DMT40.002_02674 formed a monophyletic group with DmtH, which is a known DMT-degrading enzyme (Fig. 5B). Therefore, molecular modeling and docking simulations were performed to evaluate the interaction of DMT40.002_02674, the most closely related to DmtH, and DMT40.002_0288 with the substrate. It has been reported that DmtH has a catalytic triad and degrades DMT [9]. The modeling and simulations showed that DMT40.002_02674 and DMT40.002_0288 have a binding pocket for DMT and MMT supported by hydrogen bonding, π-π stacking interactions, and hydrophobic interactions (Fig. 6B). The ester linkage of MMT allows binding near the active Ser (Ser-108 for DMT40.002_02674, Ser-58 for DMT 40.002_0288), suggesting that these enzymes can degrade MMT.

From the results of enrichment cultures and ^{1}H NMR analysis, it is clear that MMT, TA, and methanol are produced after DMT degradation, and methanol is finally converted to methane gas (Fig. 1 and Table 1). In addition, microscopic observations showed that Spirochaetota-like cells were attached to the DMT crystals (Figs. 3B and 3C), further supporting the possibility that Treponema_G (DMT40.002) may hydrolyze DMT and MMT. The most abundant microorganism, *Methanomethylovorans* (DMT6_6), possesses MtaABC and Mcr required for methanogenesis from methanol (Table S9), indicating that *Methanomethylovorans* DMT6_6 is a methanol-utilizing methanogenic archaea, as previously reported [55]. Anaerobic methanol utilization by bacteria has been confirmed in several acetogens *(e.g., A. woodii*, *Butyribacterium methylotrphicum*, and *Moorella thermoacetica*), and recently, methanol metabolism and its electron transfer via the mta operon have been revealed using *A. woodii* as a model organism [56]. A comparative analysis of the genome of Treponema_G (DMT40.002) with *A. woodii* based on blastp was performed to evaluate the presence of the mta operon, but no homologs were found, suggesting that Treponema_G (DMT40.002) does not have any known methanol utilization-related genes. In addition, Treponema_G (DMT40.002) is unlikely to be an acetogen because the core genes for acetogenesis were missing (Table 3). Based on microscopic observation, Spirochaetota-like cells frequently associated with the flocs of *Methanomethylovorans*-like coccoid cells (Figs. 3E and 3F). Because Treponema_G (DMT40.002) has genes related to amino acid and sugar metabolism (Tables S15 and S16), it grows by acquiring nutrients such as amino acids from *Methanomethylovorans*.

3.4 Summary of DMT and BHET degradation

In this study, previously unexplored anaerobic BHET and DMT-degrading microorganisms were revealed by enrichment cultures and microbiome analyses.

Interestingly, the enriched putative BHET- and DMT-degrading metagenomic bins all belonged to the phylum Spirochaeota (Cluster.64, BHET.Bin.69, BHET_244_sub, and DMT40.002). Phylum Spirochaeota is frequently found in several anaerobic bioreactors treating PTA (a raw material for PET production) manufacturing wastewater [25,57] and has been predicted to participate in dead cell-derived amino acid metabolism in the reactors [58]. To our knowledge, there are no reports that Spirochaeota can degrade PET or PET-related materials. A recent large-scale homology search using known plastic degradation genes as a reference has reported that 11 genes in the phylum Spirochaeota related to a polyhydroxyalkanoate depolymerase; however, those functions are still unknown due to the lack of biochemical experiments [59]. Although gene expression or enzymatic activity remain unexplored, this study accomplishes the observation of BHET and DMT degradation in enrichment cultures supported by combining NMR-based identification of metabolites, metagenomic analysis, and enzyme modeling and identification of uncultured Spirochaetota likely capable of hydrolyzing BHET and DMT. Further research is necessary to evaluate the activity of the identified hydrolytic enzymes.

Comparing the degradation rates of BHET and DMT with previous studies, DMT conversion rates of this study (0.096–0.27 mM-MMT-production/day, Table 2) were much higher than *Sphingobium* sp. C3 (0.03 mM/day), which possesses DmtH [9]. Furthermore, 0.025–0.091 mM-TA-production/day was observed from the DMT enrichment cultures, suggesting that the predicted DMT-degrading enzymes may also convert MMT to TA (Fig. 6), a property that DmtH lacks [9]. For BHET degradation, 0.31–0.41 mM-MHET-production/day and 0.015–0.025 mM-TA-production/day were obtained from BHET enrichment cultures of this study. A previous study reported that p-nitrobenzylesterase-related enzyme BsEstB from *B. subtilis* 4P3-11 showed faster bioconversion rate for MHET than those for TA [50]. Further investigations on the enzymatic activity of Spirochaetota-

derived enzymes are required to properly compare the degradation behavior between aerobic and anaerobic condition.

In the BHET enrichment cultures, two metagenomic bins belonging to the class Negativicutes were highly enriched, and the 16S rRNA gene analysis showed that the relative abundance of these two phylotypes (BHET001 and BHET004) accounted for 87-97% of the total prokaryotic population (Fig. 2A and Table S2) and 91% of all metagenomic bins by metagenomic analysis (BC_{7U}, Fig. 4A and Table S4). Although no 16S rRNA gene sequences were recovered from these bins (BHET.Bin.209 and BHET40.249), the closest relatives of OTUs BHET001 and BHET004 obtained by amplicon sequencing are *Methylomusa anaerophila* MMFC1 (340/378 bp, 90%, NR_163640.1) [60] and *Dendrosporobacter quercicolus* DSM 1736 (352/375 bp, 94%, NR_041949.1) [61], respectively, which are not acetogens. On the other hand, there are lineages of acetogens, such as the genera *Sporomusa* [62] and *Acetonema* [63], in the class Negativicutes; therefore, the enriched BHET.Bin.209 (BHET001) and BHET40.249 (BHET004) in this study may belong to a novel phylogenetic clade capable of acetogenesis. Furthermore, these phylotypes were respectively placed in uncultured order-level (UBA11029) and family-level (UBA7701) lineages (Table S4, referred from the GTDBtk, r202 database) and provide new physiological and genomic information these uncultured lineages. In the future, use of EG and ethanol as energy sources may allow cultivation/isolation of these putative acetogens.

Considering that most plastics, including PET, are disposed of in landfills, it is necessary to evaluate their degradability and byproducts in anaerobic as well as aerobic environments. In addition, the removal efficiency of microplastics in sewage treatment plants, which are considered to be one of the major sources of microplastic contamination in the aquatic environment, and optimal operation/infrastructure to prevent the outflow of microplastics have also been studied [64], but effective solutions have yet to be innovated.

4. Conclusions

In conclusion, this study succeeded in enrichment of BHET- and DMT-degrading microbial consortia under anaerobic conditions and showed that microorganisms belonging to the phylum Spirochaetota are capable of hydrolyzing BHET and DMT and their byproducts are utilized by Negativicutes and by *Methanomethylovorans*, respectively, through the cultivation, microbiome, and metabolome analyses. These observations can be useful for the development of anaerobic plastics-degrading bioprocess and *in situ* bioremediation strategy. Future detailed studies on the isolation of Spirochaetota and/or evaluation of hydrolytic capacities by *in vitro* expression of enzymes associated with the degradation of PET and PET-related chemicals are critical for the development of novel PET removal biotechnology.

Acknowledgments

This study was supported by the Japan Society for the Promotion of Science (JSPS) KAKENHI Grant numbers JP18H01576 and JP21H01471. The authors thank Riho Tokizawa at the National Institute of Advanced Industrial Science and Technology (AIST) and Futaba Shinshima at the National Institute of Technology, Miyakonojo College for their technical assistance. The authors also thank Ran Mei at the National Institute of Advanced Industrial Science and Technology (AIST) for stimulating discussion.

References

[1] M. Djapovic, D. Milivojevic, T. Ilic-Tomic, M. Lješević, E. Nikolaivits, E. Topakas, V. Maslak, J. Nikodinovic-Runic, Synthesis and characterization of polyethylene terephthalate (PET) precursors and potential degradation products: Toxicity study and

application in discovery of novel PETases, Chemosphere. 275 (2021) 130005. https://doi.org/10.1016/j.chemosphere.2021.130005.

[2] M. Volanti, D. Cespi, F. Passarini, E. Neri, F. Cavani, P. Mizsey, D. Fozer, Terephthalic acid from renewable sources: Early-stage sustainability analysis of a bio-PET precursor, Green Chem. 21 (2019) 885–896. https://doi.org/10.1039/c8gc03666g.

[3] E. Barnard, J.J. Rubio Arias, W. Thielemans, Chemolytic depolymerisation of PET: A review, Green Chem. 23 (2021) 3765–3789. https://doi.org/10.1039/d1gc00887k.

[4] R. Geyer, J.R. Jambeck, K.L. Law, Production, use, and fate of all plastics ever made, Sci. Adv. 3 (2017) 25–29. https://doi.org/10.1126/sciadv.1700782.

[5] A. Stubbins, K.L. Law, S.E. Muñoz, T.S. Bianchi, L. Zhu, Plastics in the Earth system., Science. 373 (2021) 51–55. https://doi.org/10.1126/science.abb0354.

[6] M.W. Kwan So, L.D. Vorsatz, S. Cannicci, C. Not, Fate of plastic in the environment: From macro to nano by macrofauna, Environ. Pollut. 300 (2022) 118920. https://doi.org/10.1016/j.envpol.2022.118920.

[7] Z.W. He, W.J. Yang, Y.X. Ren, H.Y. Jin, C.C. Tang, W.Z. Liu, C.X. Yang, A.J. Zhou, A.J. Wang, Occurrence, effect, and fate of residual microplastics in anaerobic digestion of waste activated sludge: A state-of-the-art review, Bioresour. Technol. 331 (2021) 125035. https://doi.org/10.1016/j.biortech.2021.125035.

[8] X. Li, L. Chen, Y. Ji, M. Li, B. Dong, G. Qian, J. Zhou, X. Dai, Effects of chemical pretreatments on microplastic extraction in sewage sludge and their physicochemical characteristics, Water Res. 171 (2020) 115379. https://doi.org/10.1016/j.watres.2019.115379.

[9] X. Cheng, S. Dong, D. Chen, Q. Rui, J. Guo, Dayong Wang, J. Jiang, Potential of esterase DmtH in transforming plastic additive dimethyl terephthalate to less toxic

mono-methyl terephthalate, Ecotoxicol. Environ. Saf. 187 (2020) 109848. https://doi.org/10.1016/j.ecoenv.2019.109848.

[10] I. Taniguchi, S. Yoshida, K. Hiraga, K. Miyamoto, Y. Kimura, K. Oda, Biodegradation of PET: Current Status and Application Aspects, ACS Catal. 9 (2019) 4089–4105. https://doi.org/10.1021/acscatal.8b05171.

[11] F. Kawai, T. Kawabata, M. Oda, Current State and Perspectives Related to the Polyethylene Terephthalate Hydrolases Available for Biorecycling, ACS Sustain. Chem. Eng. 8 (2020) 8894–8908. https://doi.org/10.1021/acssuschemeng.0c01638.

[12] O. Yasin, I. Zelal, D. Nadir, Acetic acid and methanol recovery from dimethyl terephthalate process wastewater using pressure membrane and membrane distillation processes, J. Water Process Eng. 38 (2020). https://doi.org/10.1016/j.jwpe.2020.101532.

[13] K.K. Garg, B. Prasad, Treatment of toxic pollutants of purified terephthalic acid waste water: A review, Environ. Technol. Innov. 8 (2017) 191–217. https://doi.org/10.1016/j.eti.2017.07.001.

[14] S. Joo, I.J. Cho, H. Seo, H.F. Son, H.Y. Sagong, T.J. Shin, S.Y. Choi, S.Y. Lee, K.J. Kim, Structural insight into molecular mechanism of poly(ethylene terephthalate) degradation, Nat. Commun. 9 (2018). https://doi.org/10.1038/s41467-018-02881-1.

[15] S. Yoshida, K. Hiraga, T. Takehana, I. Taniguchi, H. Yamaji, Y. Maeda, K. Toyohara, K. Miyamoto, Y. Kimura, K. Oda, A bacterium that degrades and assimilates poly(ethylene terephthalate), Science (80-.). 351 (2016) 1196–1199. https://doi.org/10.1126/science.aad6359.

[16] N.A. Samak, Y. Jia, M.M. Sharshar, T. Mu, M. Yang, S. Peh, J. Xing, Recent advances in biocatalysts engineering for polyethylene terephthalate plastic waste green

recycling, Environ. Int. 145 (2020) 106144. https://doi.org/10.1016/j.envint.2020.106144.

[17] I.A. Kane, M.A. Clare, E. Miramontes, R. Wogelius, J.J. Rothwell, P. Garreau, F. Pohl, Seafloor microplastic hotspots controlle by deep-sea circulation, Science (80-.). 368 (2020) 1140–1145. https://doi.org/10.1126/science.aba5899.

[18] R. Kleerebezem, L.W. Hulshoff Pol, G. Lettinga, Anaerobic biodegradability of phthalic acid isomers and related compounds, Biodegradation. 10 (1999) 63–73. https://doi.org/10.1023/A:1008321015498.

[19] Y.-L. Qiu, Y. Sekiguchi, S. Hanada, H. Imachi, I.-C. Tseng, S.-S. Cheng, A. Ohashi, H. Harada, Y. Kamagata, Pelotomaculum terephthalicum sp. nov. and Pelotomaculum isophthalicum sp. nov.: two anaerobic bacteria that degrade phthalate isomers in syntrophic association with hydrogenotrophic methanogens, Arch. Microbiol. 185 (2006) 172–182. https://doi.org/10.1007/s00203-005-0081-5.

[20] Y.L. Qiu, S. Hanada, A. Ohashi, H. Harada, Y. Kamagata, Y. Sekiguchi, Syntrophorhabdus aromaticivorans gen. nov., sp. nov., the first cultured anaerobe capable of degrading phenol to acetate in obligate syntrophic associations with a hydrogenotrophic methanogen, Appl. Environ. Microbiol. 74 (2008) 2051–2058. https://doi.org/10.1128/AEM.02378-07.

[21] F. Yan, R. Wei, Q. Cui, U.T. Bornscheuer, Y.J. Liu, Thermophilic whole-cell degradation of polyethylene terephthalate using engineered Clostridium thermocellum, Microb. Biotechnol. 14 (2021) 374–385. https://doi.org/10.1111/1751-7915.13580.

[22] K. Kuroda, T. Narihiro, F. Shinshima, M. Yoshida, H. Yamaguchi, H. Kurashita, N. Nakahara, M.K. Nobu, T.Q.P. Noguchi, M. Yamauchi, M. Yamada, High-rate cotreatment of purified terephthalate and dimethyl terephthalate manufacturing wastewater by a mesophilic upflow anaerobic sludge blanket reactor and the microbial

ecology relevant to aromatic compound degradation, Water Res. 219 (2022) 118581. https://doi.org/10.1016/j.watres.2022.118581.

[23] T. Narihiro, M.K. Nobu, N.-K. Kim, Y. Kamagata, W.-T. Liu, The nexus of syntrophy-associated microbiota in anaerobic digestion revealed by long-term enrichment and community survey, Environ. Microbiol. 17 (2015) 1707–1720. https://doi.org/10.1111/1462-2920.12616.

[24] J.J. Kozich, S.L. Westcott, N.T. Baxter, S.K. Highlander, P.D. Schloss, Development of a Dual-Index Sequencing Strategy and Curation Pipeline for Analyzing Amplicon Sequence Data on the MiSeq Illumina Sequencing Platform, Appl. Environ. Microbiol. 79 (2013) 5112–5120. https://doi.org/10.1128/AEM.01043-13.

[25] K. Kuroda, M.K. Nobu, R. Mei, T. Narihiro, B.T.W. Bocher, T. Yamaguchi, W.-T. Liu, A single-granule-level approach reveals ecological heterogeneity in an upflow anaerobic sludge blanket reactor, PLoS One. 11 (2016). https://doi.org/10.1371/journal.pone.0167788.

[26] E. Bolyen, J.R. Rideout, M.R. Dillon, N.A. Bokulich, C.C. Abnet, G.A. Al-Ghalith, H. Alexander, E.J. Alm, M. Arumugam, F. Asnicar, Y. Bai, J.E. Bisanz, K. Bittinger, A. Brejnrod, C.J. Brislawn, C.T. Brown, B.J. Callahan, A.M. Caraballo-Rodríguez, J. Chase, E.K. Cope, R. Da Silva, C. Diener, P.C. Dorrestein, G.M. Douglas, D.M. Durall, C. Duvallet, C.F. Edwardson, M. Ernst, M. Estaki, J. Fouquier, J.M. Gauglitz, S.M. Gibbons, D.L. Gibson, A. Gonzalez, K. Gorlick, J. Guo, B. Hillmann, S. Holmes, H. Holste, C. Huttenhower, G.A. Huttley, S. Janssen, A.K. Jarmusch, L. Jiang, B.D. Kaehler, K. Bin Kang, C.R. Keefe, P. Keim, S.T. Kelley, D. Knights, I. Koester, T. Kosciolek, J. Kreps, M.G.I. Langille, J. Lee, R. Ley, Y.-X. Liu, E. Loftfield, C. Lozupone, M. Maher, C. Marotz, B.D. Martin, D. McDonald, L.J. McIver, A. V. Melnik, J.L. Metcalf, S.C. Morgan, J.T. Morton, A.T. Naimey, J.A. Navas-Molina,

L.F. Nothias, S.B. Orchanian, T. Pearson, S.L. Peoples, D. Petras, M.L. Preuss, E. Pruesse, L.B. Rasmussen, A. Rivers, M.S. Robeson, P. Rosenthal, N. Segata, M. Shaffer, A. Shiffer, R. Sinha, S.J. Song, J.R. Spear, A.D. Swafford, L.R. Thompson, P.J. Torres, P. Trinh, A. Tripathi, P.J. Turnbaugh, S. Ul-Hasan, J.J.J. van der Hooft, F. Vargas, Y. Vázquez-Baeza, E. Vogtmann, M. von Hippel, W. Walters, Y. Wan, M. Wang, J. Warren, K.C. Weber, C.H.D. Williamson, A.D. Willis, Z.Z. Xu, J.R. Zaneveld, Y. Zhang, Q. Zhu, R. Knight, J.G. Caporaso, Reproducible, interactive, scalable and extensible microbiome data science using QIIME 2, Nat. Biotechnol. 37 (2019) 852–857. https://doi.org/10.1038/s41587-019-0209-9.

[27] B.J. Callahan, P.J. McMurdie, M.J. Rosen, A.W. Han, A.J.A. Johnson, S.P. Holmes, DADA2: High-resolution sample inference from Illumina amplicon data, Nat. Methods. 13 (2016) 581–583. https://doi.org/10.1038/nmeth.3869.

[28] T. Rognes, T. Flouri, B. Nichols, C. Quince, F. Mahé, VSEARCH: a versatile open source tool for metagenomics, PeerJ. 4 (2016) e2584. https://doi.org/10.7717/peerj.2584.

[29] P. Yilmaz, L.W. Parfrey, P. Yarza, J. Gerken, E. Pruesse, C. Quast, T. Schweer, J. Peplies, W. Ludwig, F.O. Glöckner, The SILVA and "All-species Living Tree Project (LTP)" taxonomic frameworks, Nucleic Acids Res. 42 (2014) D643–D648. https://doi.org/10.1093/nar/gkt1209.

[30] A.M. Bolger, M. Lohse, B. Usadel, Trimmomatic: a flexible trimmer for Illumina sequence data, Bioinformatics. 30 (2014) 2114–2120. https://doi.org/10.1093/bioinformatics/btu170.

[31] D. Li, C.-M. Liu, R. Luo, K. Sadakane, T.-W. Lam, MEGAHIT: an ultra-fast single-node solution for large and complex metagenomics assembly via succinct de Bruijn

graph, Bioinformatics. 31 (2015) 1674–1676. https://doi.org/10.1093/bioinformatics/btv033.

[32] D.D. Kang, F. Li, E. Kirton, A. Thomas, R. Egan, H. An, Z. Wang, MetaBAT 2: an adaptive binning algorithm for robust and efficient genome reconstruction from metagenome assemblies, PeerJ. 7 (2019) e7359. https://doi.org/10.7717/peerj.7359.

[33] Y.-W. Wu, B.A. Simmons, S.W. Singer, MaxBin 2.0: an automated binning algorithm to recover genomes from multiple metagenomic datasets, Bioinformatics. 32 (2016) 605–607. https://doi.org/10.1093/bioinformatics/btv638.

[34] H.-H. Lin, Y.-C. Liao, Accurate binning of metagenomic contigs via automated clustering sequences using information of genomic signatures and marker genes, Sci. Rep. 6 (2016) 24175. https://doi.org/10.1038/srep24175.

[35] J.N. Nissen, J. Johansen, R.L. Allesøe, C.K. Sønderby, J.J.A. Armenteros, C.H. Grønbech, L.J. Jensen, H.B. Nielsen, T.N. Petersen, O. Winther, S. Rasmussen, Improved metagenome binning and assembly using deep variational autoencoders, Nat. Biotechnol. 39 (2021) 555–560. https://doi.org/10.1038/s41587-020-00777-4.

[36] C.M.K. Sieber, A.J. Probst, A. Sharrar, B.C. Thomas, M. Hess, S.G. Tringe, J.F. Banfield, Recovery of genomes from metagenomes via a dereplication, aggregation and scoring strategy, Nat. Microbiol. 3 (2018) 836–843. https://doi.org/10.1038/s41564-018-0171-1.

[37] M.R. Olm, C.T. Brown, B. Brooks, J.F. Banfield, dRep: a tool for fast and accurate genomic comparisons that enables improved genome recovery from metagenomes through de-replication, ISME J. 11 (2017) 2864–2868. https://doi.org/10.1038/ismej.2017.126.

[38] T. Seemann, Prokka: rapid prokaryotic genome annotation, Bioinformatics. 30 (2014) 2068–2069. https://doi.org/10.1093/bioinformatics/btu153.

[39] M. Kanehisa, Y. Sato, K. Morishima, BlastKOALA and GhostKOALA: KEGG Tools for Functional Characterization of Genome and Metagenome Sequences, J. Mol. Biol. 428 (2016) 726–731. https://doi.org/10.1016/j.jmb.2015.11.006.

[40] M. Shaffer, M.A. Borton, B.B. McGivern, A.A. Zayed, S.L. La Rosa, L.M. Solden, P. Liu, A.B. Narrowe, J. Rodríguez-Ramos, B. Bolduc, M.C. Gazitúa, R.A. Daly, G.J. Smith, D.R. Vik, P.B. Pope, M.B. Sullivan, S. Roux, K.C. Wrighton, DRAM for distilling microbial metabolism to automate the curation of microbiome function, Nucleic Acids Res. 48 (2020) 8883–8900. https://doi.org/10.1093/nar/gkaa621.

[41] H. Nordberg, M. Cantor, S. Dusheyko, S. Hua, A. Poliakov, I. Shabalov, T. Smirnova, I. V. Grigoriev, I. Dubchak, The genome portal of the Department of Energy Joint Genome Institute: 2014 updates, Nucleic Acids Res. 42 (2014) D26–D31. https://doi.org/10.1093/nar/gkt1069.

[42] K. Katoh, D.M. Standley, MAFFT Multiple Sequence Alignment Software Version 7: Improvements in Performance and Usability, Mol. Biol. Evol. 30 (2013) 772–780. https://doi.org/10.1093/molbev/mst010.

[43] B.Q. Minh, H.A. Schmidt, O. Chernomor, D. Schrempf, M.D. Woodhams, A. Von Haeseler, R. Lanfear, E. Teeling, IQ-TREE 2: New Models and Efficient Methods for Phylogenetic Inference in the Genomic Era, Mol. Biol. Evol. 37 (2020) 1530–1534. https://doi.org/10.1093/molbev/msaa015.

[44] P.-A. Chaumeil, A.J. Mussig, P. Hugenholtz, D.H. Parks, GTDB-Tk: a toolkit to classify genomes with the Genome Taxonomy Database, Bioinformatics. 36 (2019) 1925–1927. https://doi.org/10.1093/bioinformatics/btz848.

[45] J. Jumper, R. Evans, A. Pritzel, T. Green, M. Figurnov, O. Ronneberger, K. Tunyasuvunakool, R. Bates, A. Žídek, A. Potapenko, A. Bridgland, C. Meyer, S.A.A. Kohl, A.J. Ballard, A. Cowie, B. Romera-Paredes, S. Nikolov, R. Jain, J. Adler, T.

Back, S. Petersen, D. Reiman, E. Clancy, M. Zielinski, M. Steinegger, M. Pacholska, T. Berghammer, S. Bodenstein, D. Silver, O. Vinyals, A.W. Senior, K. Kavukcuoglu, P. Kohli, D. Hassabis, Highly accurate protein structure prediction with AlphaFold, Nature. 596 (2021) 583–589. https://doi.org/10.1038/s41586-021-03819-2.

[46] E.F. Pettersen, T.D. Goddard, C.C. Huang, G.S. Couch, D.M. Greenblatt, E.C. Meng, T.E. Ferrin, UCSF Chimera–A visualization system for exploratory research and analysis, J. Comput. Chem. 25 (2004) 1605–1612. https://doi.org/10.1002/jcc.20084.

[47] O. Trott, A.J. Olson, AutoDock Vina: Improving the speed and accuracy of docking with a new scoring function, efficient optimization, and multithreading, J. Comput. Chem. 31 (2009) NA-NA. https://doi.org/10.1002/jcc.21334.

[48] Z.-W. He, Z.-S. Zou, Q. Sun, H.-Y. Jin, X.-Y. Yao, W.-J. Yang, C.-C. Tang, A.-J. Zhou, W. Liu, Y.-X. Ren, A. Wang, Freezing-low temperature treatment facilitates short-chain fatty acids production from waste activated sludge with short-term fermentation, Bioresour. Technol. 347 (2022) 126337. https://doi.org/10.1016/j.biortech.2021.126337.

[49] H. Imachi, Y. Sekiguchi, Y. Kamagata, S. Hanada, Pelotomaculum thermopropionicum gen . nov ., sp . nov ., an anaerobic , thermophilic , syntrophic propionate-oxidizing bacterium, Int. J. Syst. Evol. Microbiol. (2002) 1729–1735. https://doi.org/10.1099/ijs.0.02212-0.Abbreviations.

[50] D. Ribitsch, S. Heumann, E. Trotscha, E. Herrero Acero, K. Greimel, R. Leber, R. Birner-Gruenberger, S. Deller, I. Eiteljoerg, P. Remler, T. Weber, P. Siegert, K.H. Maurer, I. Donelli, G. Freddi, H. Schwab, G.M. Guebitz, Hydrolysis of polyethyleneterephthalate by p-nitrobenzylesterase from Bacillus subtilis, Biotechnol. Prog. 27 (2011) 951–960. https://doi.org/10.1002/btpr.610.

[51] H. Imachi, Y. Sekiguchi, Y. Kamagata, S. Hanada, A. Ohashi, H. Harada, Pelotomaculum thermopropionicum gen. nov., sp. nov., an anaerobic, thermophilic, syntrophic propionate-oxidizing bacterium., Int. J. Syst. Evol. Microbiol. 52 (2002) 1729–1735. https://doi.org/10.1099/00207713-52-5-1729.

[52] D. Trifunović, K. Schuchmann, V. Müller, Ethylene glycol metabolism in the acetogen Acetobacterium woodii, J. Bacteriol. 198 (2016) 1058–1065. https://doi.org/10.1128/JB.00942-15.

[53] N.P. Chowdhury, L. Alberti, M. Linder, V. Müller, Exploring Bacterial Microcompartments in the Acetogenic Bacterium Acetobacterium woodii, Front. Microbiol. 11 (2020). https://doi.org/10.3389/fmicb.2020.593467.

[54] J. Bertsch, A.L. Siemund, F. Kremp, V. Müller, A novel route for ethanol oxidation in the acetogenic bacterium Acetobacterium woodii: the acetaldehyde/ethanol dehydrogenase pathway, Environ. Microbiol. 18 (2016) 2913–2922. https://doi.org/10.1111/1462-2920.13082.

[55] K.C. Costa, J.A. Leigh, Metabolic versatility in methanogens, Curr. Opin. Biotechnol. 29 (2014) 70–75. https://doi.org/10.1016/j.copbio.2014.02.012.

[56] F. Kremp, A. Poehlein, R. Daniel, V. Müller, Methanol metabolism in the acetogenic bacterium Acetobacterium woodii, Environ. Microbiol. 20 (2018) 4369–4384. https://doi.org/10.1111/1462-2920.14356.

[57] T. Narihiro, M.K. Nobu, B.T.W. Bocher, R. Mei, W.T. Liu, Co-occurrence network analysis reveals thermodynamics-driven microbial interactions in methanogenic bioreactors, Environ. Microbiol. Rep. 10 (2018) 673–685. https://doi.org/10.1111/1758-2229.12689.

[58] M.K. Nobu, T. Narihiro, C. Rinke, Y. Kamagata, S.G. Tringe, T. Woyke, W. Liu, Microbial dark matter ecogenomics reveals complex synergistic networks in a

methanogenic bioreactor, ISME J. 9 (2015) 1710–1722. https://doi.org/10.1038/ismej.2014.256.

[59] V. Gambarini, O. Pantos, J.M. Kingsbury, L. Weaver, K.M. Handley, G. Lear, Phylogenetic Distribution of Plastic-Degrading Microorganisms, MSystems. 6 (2021). https://doi.org/10.1128/msystems.01112-20.

[60] N. Amano, A. Yamamuro, M. Miyahara, A. Kouzuma, T. Abe, K. Watanabe, Methylomusa anaerophila gen. Nov., sp. nov., an anaerobic methanol-utilizing bacterium isolated from a microbial fuel cell, Int. J. Syst. Evol. Microbiol. 68 (2018) 1118–1122. https://doi.org/10.1099/ijsem.0.002635.

[61] C. Strömpl, B.J. Tindall, H. Lünsdorf, T.Y. Wong, E.R.B. Moore, H. Hippe, Reclassification of Clostridium quercicolum as Dendrosporobacter quercicolus gen. nov., comb. nov., Int. J. Syst. Evol. Microbiol. 50 (2000) 101–106. https://doi.org/10.1099/00207713-50-1-101.

[62] B. Möller, R. Oßmer, B.H. Howard, G. Gottschalk, H. Hippe, Sporomusa, a new genus of gram-negative anaerobic bacteria including Sporomusa sphaeroides spec. nov. and Sporomusa ovata spec. nov., Arch. Microbiol. 139 (1984) 388–396. https://doi.org/10.1007/BF00408385.

[63] M.D. Kane, J.A. Breznak, Acetonema longum gen.nov.sp.nov., an H2/CO2 acetogenic bacterium from the termite, Pterotermes occidentis, Arch. Microbiol. 156 (1991) 91–98. https://doi.org/10.1007/BF00290979.

[64] W. Liu, J. Zhang, H. Liu, X. Guo, X. Zhang, X. Yao, Z. Cao, T. Zhang, A review of the removal of microplastics in global wastewater treatment plants: Characteristics and mechanisms, Environ. Int. 146 (2021) 106277. https://doi.org/10.1016/j.envint.2020.106277.

Supplementary Tables

Table S1. Summary of the sampling days of the bis(2-hydroxyethyl) terephthalate (BHET) and dimethyl terephthalate (DMT) enrichment cultures.

Table S2. Relative abundance (%) of bis(2-hydroxyethyl) terephthalate (BHET) enrichment cultures based on 16S rRNA gene amplicon sequencing

Table S3. Relative abundance (%) of dimethyl terephthalate (DMT) enrichment cultures based on 16S rRNA gene amplicon sequencing

Table S4. Summary of the metagenomic bins from BHET enrichment cultures observed in this study

Table S5. Summary of the metagenomic bins from the DC_{7A} observed in this study

Table S6. Average nucleotide identity (ANI) based on the goANI algorithm between metagenomic bins from BHET and DMT enrichment cultures

Table S7. Amino acid identity to known proteins of the genes annotated in putative bis(2-hydroxyethyl) terephthalate or dimethyl terephthalate-degrading bins

Table S8. Sequence alignment of putative BHET hydrolases with their closely related known PET- or MHET-degrading genes

Table S9. Locus tags for genes encoding methanogenesis from hydrogen, formate, methanol, and acetate in this study

Table S10. Sequence alignment of putative DmtH with their closely related known DMT-degrading genes

Table S11. Locus tags for genes encoding ethylene glycol-related metabolisms in this study at the thresholds ≤1e-5 to genes of Acetobacterium woodii

Table S12. Amino acid identity to known proteins of the bacterial microcompartments (BMC)-related genes annotated in the bins of putative bis(2-hydroxyethyl) terephthalate enrichment cultures

Table S13. Locus tags for genes encoding ethanol and formate-related metabolisms in this study at the thresholds as ≤1e-5 to genes of Acetobacterium woodii

Table S14. Amino acid identity to known proteins of the alcohol and formate metabolism-related genes annotated in the bins of putative bis(2-hydroxyethyl) terephthalate enrichment cultures

Table S15. Summary of the annotation of Negativicutes and Spirochaeota bins based on BlastKOALA in the KEGG database

Table S16. Summary of the annotation of BHET- or DMT-degrading Spiroarchaeota bins using DRAM annotation software